



City Research Online

City, University of London Institutional Repository

Citation: Gong, J., Li, Y., Yan, S. & Ma, Q. (2022). Numerical simulation of turn and zigzag Maneuvres of trimaran in calm water and waves by a hybrid method. *Ocean Engineering*, 253, 111239. doi: 10.1016/j.oceaneng.2022.111239

This is the accepted version of the paper.

This version of the publication may differ from the final published version.

Permanent repository link: <https://openaccess.city.ac.uk/id/eprint/29078/>

Link to published version: <https://doi.org/10.1016/j.oceaneng.2022.111239>

Copyright: City Research Online aims to make research outputs of City, University of London available to a wider audience. Copyright and Moral Rights remain with the author(s) and/or copyright holders. URLs from City Research Online may be freely distributed and linked to.

Reuse: Copies of full items can be used for personal research or study, educational, or not-for-profit purposes without prior permission or charge. Provided that the authors, title and full bibliographic details are credited, a hyperlink and/or URL is given for the original metadata page and the content is not changed in any way.

City Research Online:

<http://openaccess.city.ac.uk/>

publications@city.ac.uk

Numerical Simulation of Turn and Zigzag Maneuvres of Trimaran in Calm Water and Waves by a Hybrid Method

Jiaye Gong¹, Yunbo Li^{1*}, Shiqiang Yan², Qingwei Ma²

1. College of Ocean Science and Engineering, Shanghai Maritime University, China

2. School of Mathematics, Computer Science and Engineering, City, University of London, UK

*Corresponding Author: liybsmu@163.com

Abstract: As one of the widely used high-performance ships, the hydrodynamic characteristics of the trimaran ships have been widely investigated in recent years. But, the study on the maneuverability and the skill of the maneuvering simulation are still limited. In this paper, a hybrid method coupling the FNPT-based (fully nonlinear potential flow theory) QALE-FEM (quasi arbitrary Lagrangian-Eulerian finite element method) with the viscous flow method is applied to simulate the turn and zigzag maneuvers of the trimaran in both calm water and waves. The environment of calm water and incident waves is simulated by the numerical tank of QALE-FEM. The maneuvering of the trimaran is carried out in the scope of the numerical tank by the viscous flow method. The grid convergence test is carried out first, and the computed results are compared with the experimental results. Then, the turn and zigzag maneuvers of a trimaran model in both calm water and waves are simulated to study the trimaran's maneuvering characteristics.

Key Words: trimaran; hybrid method; maneuver; calm water; wave.

1 Introduction

In the past decades, the hydrodynamic performance of the trimaran form has attracted more and more attention from researchers. The corresponding investigation has been widely carried out, especially for the resistance performance in calm water and the seakeeping performance in waves. For the resistance performance of the trimaran in calm water, the study began as early as twenty years ago, both the numerical method and the resistance characteristics of the trimaran with different side-hull arrangements have been well studied (Li *et al.*, 2007; Deng *et al.*, 2015; Wang *et al.*, 2021). In the past ten years, with the development of computer science and state-of-the-art numerical solvers, the added resistance and motion of the trimaran in waves of different headings has been widely investigated by both numerical simulation and tank test (Deng *et al.*, 2016, 2019; Ghadimi *et al.*, 2021; Nowruzi *et al.*, 2020; Gong *et al.*, 2020b, 2021; Fu *et al.*, 2021).

1
2 However, the study on trimaran's maneuverability is still limited, which is important for
3 hydrodynamic performance. [Yasukawa et al. \(2005\)](#) investigated the effect of side-hull positions on
4 the hydrodynamic derivatives and turn maneuver of the trimaran form by captive model test, and it
5 was found that shifting the side hulls rearward could lead to larger lateral resistance at the stern part
6 and increase the turning circle. [Javanmardi et al. \(2008\)](#) developed a CFD code for the hydrodynamic
7 simulations of the turn maneuver. With the CFD code, the resistance and maneuvering of a trimaran
8 were simulated with the viscous flow method coupled with the rigid body motion, and the computed
9 results were compared with the experimental results. [Katayama et al. \(2009\)](#) studied the maneuvering
10 motion of a trimaran form with the hydrodynamic derivatives obtained from the captive model test,
11 and the hull attitude was taken into account during the oblique towing test. [Cui et al. \(2012\)](#) applied
12 the MMG method to simulate the turn maneuver of a composite trimaran model. The turning
13 performance with different rudders is tested. [Aram et al. \(2016\)](#) applied the CFD method and an in-
14 house CFD framework to simulate the maneuvering performance of a trimaran propelled by three
15 water-jet impetus. The water-jet inlet and duct geometry are included in the simulation, and a body
16 force model is applied to replace the water-jet pump. The integral momentum theorem replaces the
17 deflection of the steering nozzles. The computed results of the zigzag maneuvers are compared with
18 the experimental results. [Jiang et al. \(2021\)](#) carried out a series of field tests to study the
19 maneuverability of a self-propulsion water-jet trimaran. The effect of the side-hull position on the
20 turn and zigzag maneuvers of a trimaran was analyzed.

21 From the literature, it could be found that the study on the maneuverability of trimaran is mainly
22 based on the captive model test and the self-propulsion model test. For most of the cases, the hull
23 attitude is not taken into account. The study about the free-running maneuver of the trimaran in calm
24 water is limited, and there are still no papers on the maneuverability of the trimaran in waves
25 published. So, more work is still necessary for the maneuverability of the trimaran. By the reference
26 ([Cui et al., 2012](#)), it is considered that the hull attitude could probably be negligible for the
27 conventional low-speed monohulls, but, for the high-speed trimaran form, the hull attitude plays a
28 vital role in the maneuverability. In the previous work ([Gong et al., 2019, 2020a](#)), it is also found that
29 taking the hull altitude into account could significantly affect the simulation of the turn and zigzag
30 maneuvers of the trimaran especially at a high Froude number. Hence, we could expect that it is
31 essential to take all the nonlinear phenomena into account for the simulation of trimaran's maneuvers
32 in calm water and waves, such as roll-pitch coupled motion, side-hull emergence, bow diving, et al.

33 In this paper, the maneuverability of the trimaran in both calm water and waves is studied by

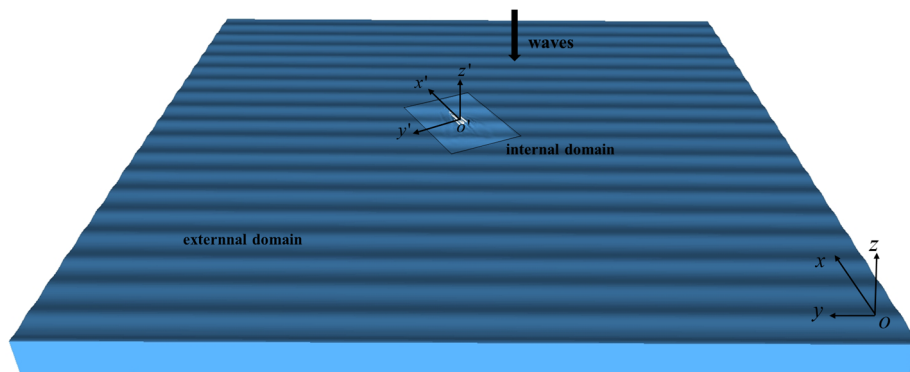
144 numerical simulation. A hybrid method coupling the FNPT and viscous flow method is applied for
2
345 numerical simulation. An external domain by FNPT-based QALE-FEM (Ma *et al.*, 2015) is used to
4
546 simulate a numerical tank, and the motion of the trimaran and the flow field near the ship are solved
6
747 by the CFD method in the internal domain. The two domains are connected by a transition zone and
8
948 interfaces. The hybrid solver for maneuvering simulation is developed based on the open source CFD
10
1149 tool OpenFOAM and the previously presented solver QaleFOAM (Li *et al.*, 2018; Yan *et al.*, 2019;
12
1350 Gong *et al.*, 2020b). The convergence test and validation of the numerical method are carried out first.
14
1551 Then, the turn and zigzag maneuvers of a trimaran in calm water at different speeds are simulated.
16
1752 Finally, the maneuvers of the trimaran in regular waves of various wavelengths and wave steepness
18
1953 are simulated, where the ship is in head waves at the beginning of the simulation. By the computed
20
2154 result, the characteristics of the maneuverability of the trimaran are analyzed.

2355 2 Numerical methods

24
25
2656 The numerical method for the maneuver simulation of the trimaran is briefly introduced in this
27
2857 section first. Then, the boundary condition and the grid generation are introduced.

3058 2.1 Hybrid method

31
32
3359 The hybrid method coupling the FNPT-based QALE-FEM and the viscous flow method has been
34
3560 presented in previous work (Li *et al.*, 2018) and has been applied to predict the seakeeping
36
3761 performance of the trimaran (Gong *et al.*, 2020b; Gong *et al.*, 2021a) and the interaction between
38
3962 focusing wave and moving cylinder (Gong *et al.*, 2021b). Hence, the hybrid method is just briefly
40
4163 introduced here for the completeness of the paper. The domain is composed of external and internal
42
4364 domains for the hybrid method, as shown in Fig. 1. The external domain is used to simulate a tank
44
4565 for the calm water or the incident wave, while the internal domain simulates the maneuver of the
46
4766 trimaran and the wave-ship interaction.



6067
6168 Fig. 1. The sketch of the hybrid method.
62
63
64
65

As shown in Fig. 1, two coordinate systems are used in the hybrid method. Both the external and internal domains are solved in the global coordinate system $o-xyz$, where the origin o is located on the surface of calm water. The x -axis is contrary to the incident wave, and the z -axis is upright. Therefore, the wave heading $\beta=180^\circ$ means the head wave in this paper. The local coordinate system $o'-x'y'z'$ is used to solve the trimaran's maneuver and motion, where the origin o' is in the gravity center of the trimaran, the x' -axis points to the bow, the y' -axis points to the portside. During the process of turn and zigzag maneuvers, the local coordinate system moves together with the trimaran.

In the external domain (Ma *et al.*, 2015; Yan *et al.*, 2019), the flow is considered incompressible, inviscid, and irrotational. The external domain is fixed in the global coordinate system, and the ship moves in the external domain. There are only incident waves simulated in this paper, so the velocity potential of the flow field is equal to the velocity potential of the wave. Both the kinematic and dynamic condition is satisfied on the free surface, and the Lagrangian method is applied to keep the free surface nodes moving simultaneously with the flow particle. The wave velocity potential satisfies the Laplace equation, the boundary condition on the self-adaption wavemaker and wave-absorber, the left, right, and bottom boundary condition, and the free surface condition. The details about the hybrid method and QaleFOAM could be found in the previous work (Ma *et al.*, 2015; Yan *et al.*, 2019; Gong *et al.*). The internal domain is discretized by the finite volume method, and the viscous flow method is used to solve the flow field, where the flow satisfies the conservation of mass and momentum. Hence, the internal domain is solved by the unsteady incompressible Navier-Stokes equations, and the volume of fluid method is applied to capture the free surface between air and water.

2.2 The maneuver motion

For both calm water and waves, the trimaran model is sailing freely with the 6DOF motion taken into account, including surge, sway, heave, roll, pitch, and yaw. When the simulation begins, the ship is upright and advances with a constant speed along the x -direction. All these can be seen in Fig. 2, where U_s is the velocity of the trimaran.

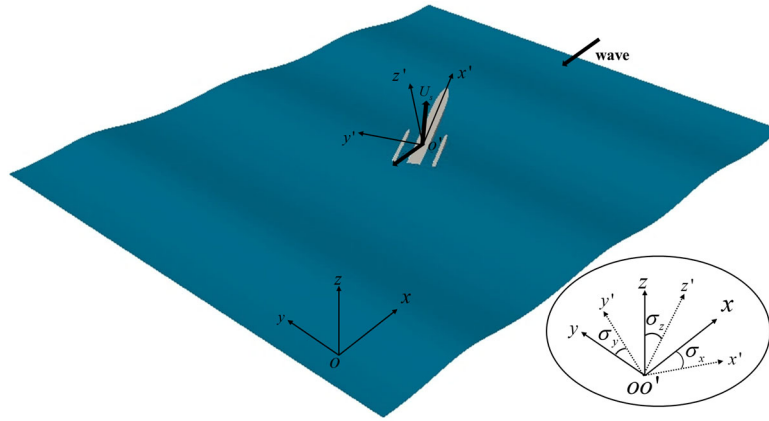


Fig. 2. The sketch of the ship motion

The motion of a ship could be divided into linear motion and rotation of the ship. The velocity and the acceleration velocity in the local are $\mathbf{U}_s=(u_{x'}, u_{y'}, u_{z'})$ and $\mathbf{a}=(\dot{u}_{x'}, \dot{u}_{y'}, \dot{u}_{z'})$. The angular velocity in the local coordinate system is $\mathbf{r}=(r_{x'}, r_{y'}, r_{z'})$. The motion of the trimaran is solved in the local coordinate system

$$\begin{aligned}
 m(\dot{u}_{x'} - u_{y'}r_{z'} + u_{z'}r_{y'}) &= F_{x'} \\
 m(\dot{v}_{y'} - u_{z'}r_{x'} + u_{x'}r_{z'}) &= F_{y'} \\
 m(\dot{w}_{z'} - u_{x'}r_{y'} + u_{y'}r_{x'}) &= F_{z'} \\
 I_{x'}r_{x'} + (I_{z'} - I_{y'})r_{y'}r_{z'} &= M_{x'} \\
 I_{y'}r_{y'} + (I_{x'} - I_{z'})r_{x'}r_{z'} &= M_{y'} \\
 I_{z'}r_{z'} + (I_{y'} - I_{x'})r_{x'}r_{y'} &= M_{z'}
 \end{aligned} \tag{1}$$

Where m is the mass of trimaran, $(I_{x'}, I_{y'}, I_{z'})$ is the inertial moment, $(F_{x'}, F_{y'}, F_{z'})$ and $(M_{x'}, M_{y'}, M_{z'})$ are the hydrodynamic force and moment. In this paper, the Euler angle $\boldsymbol{\sigma}=(\sigma_x, \sigma_y, \sigma_z)$ is used to describe the rotation of the trimaran, such as roll, pitch, and yaw. As shown in Fig. 2, the Euler angle is between the global coordinate and the local coordinate. Hence, the \mathbf{r} obtained by Eq. (1) should be transferred to the global coordinate system to obtain the change rate of $\boldsymbol{\sigma}$

$$\dot{\boldsymbol{\sigma}} = \begin{bmatrix} 1 & \sin \sigma_x \tan \sigma_y & \cos \sigma_x \tan \sigma_y \\ 0 & \cos \sigma_x & -\sin \sigma_x \\ 0 & \sin \sigma_x / \cos \sigma_y & \cos \sigma_x / \cos \sigma_y \end{bmatrix} \mathbf{r} \tag{2}$$

On the right side of Eq. (1), the total force and moment of the trimaran could be divided into the hydrodynamic ones and the propulsion ones. The hydrodynamic force and moment are obtained by solving the flow field in the internal domain. Based on the reference (Jong et al., 2012), the trimaran is powered by the water-jet impetus. A semi-empirical water jet model is used in this paper to obtain the propulsion force and moment, where the interaction between the impetus and the hull surface is

not considered.

2.3 Grid generation and boundary conditions

The size and grid generation of the external domain could be found in reference (Ma *et al.*, 2015; Yan *et al.*, 2019). In this paper, it is necessary to make sure the turn and zigzag maneuvers of the trimaran are within the scope of the external domain. Because the hybrid method has been applied to predict the seakeeping performance of the trimaran (Gong *et al.*, 2020b, 2021a), the computational domain for maneuvering simulation is similar to the one for seakeeping performance. The difference is that the grid is only refined to the direction of wave propagation for the seakeeping simulation. Still, the grid should be refined in the xy -plane for the maneuvering simulation because the wave heading is changing during the maneuvers.

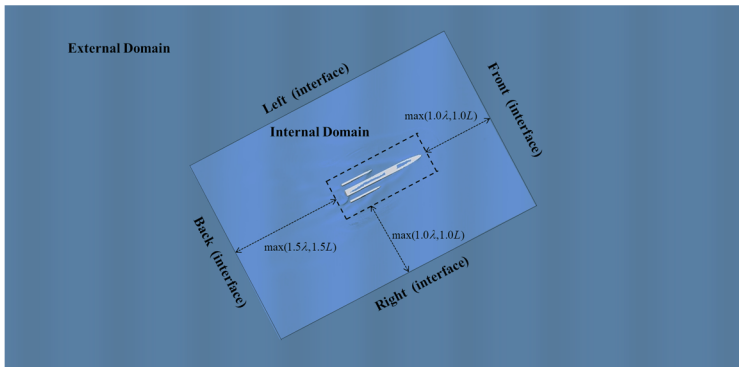


Fig. 3. The sketch of the domain for maneuvering simulation

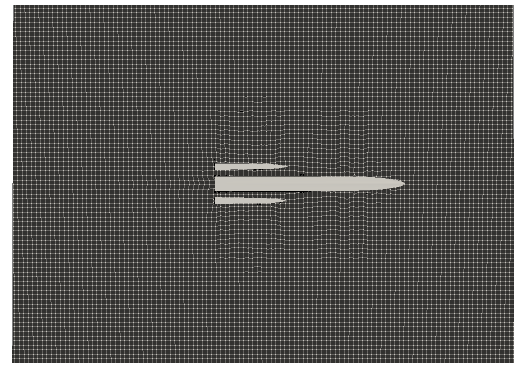


Fig. 4. The sketch of the grid of the internal domain

The grid is generated by snappyHexMesh, which is a preprocess utility in OpenFOAM. Fig. 3 shows the domain for maneuvering simulation, where λ is the wavelength, L is the waterline length. The external domain is fixed, and the internal domain moves together with the trimaran in the xy -plane. The grid near the hull surface is shown in Fig. 4. During the numerical simulation, except the top boundary, all the other boundaries of the internal domain are defined as interfaces, where the velocity is assigned by the external domain in every timestep. The regions near the front, back, left, and right are set as the transition zone. Compared with seakeeping performance, all the four boundaries will probably face the incident waves and the wake of the wave-making of the trimaran, so the length of the transition zone is the same for the four boundaries, which is 0.5λ in this paper.

3 Validation and verification

Before the numerical simulation, the convergence test and validation of the numerical method are carried out first. For the trimaran, the main dimensions of the center hull are $B/L=0.08$, $D/L=0.04$,

$C_b=0.52$, while the main dimensions of the side hull are $B_1/L_1=0.05$, $D_1/L_1=0.04$, $C_{b1}=0.46$. The $x_g/L=-0.15$, $y_g/L=0$, and $z_g/L=0.02$ are the gravity center of the trimaran. The $d_1/L=0.1$ and $d_2/L=0$ are the side-hull position, where the definition of the physical value could be found in Fig. 5.

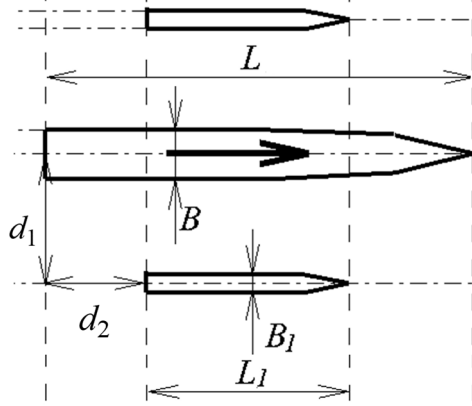
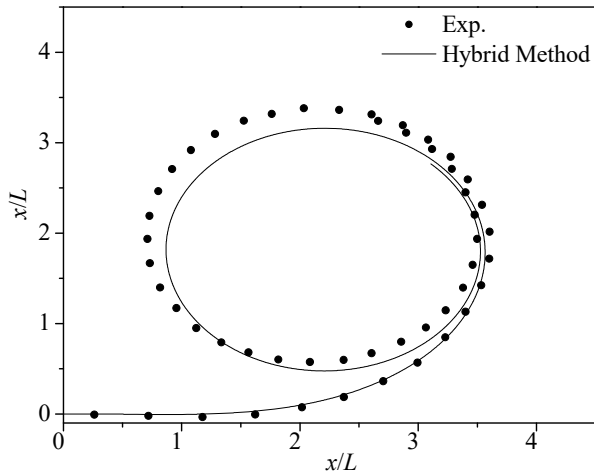
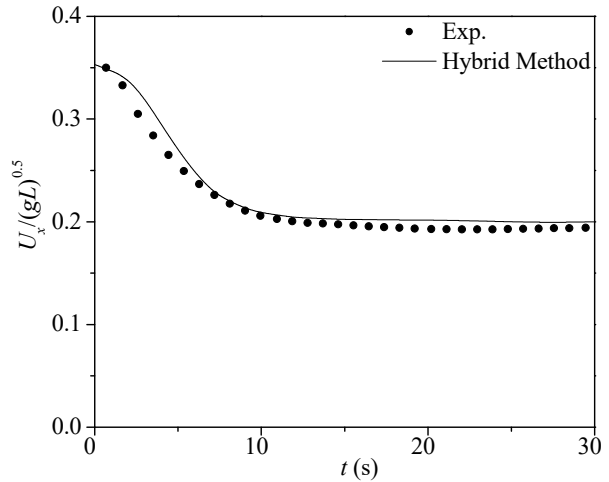


Fig. 5. The sketch of a trimaran and the dimensions

The numerical simulation of the wave generation and the trimaran's motion in waves has been validated in previous work (Gong et al., 2020b, 2021a). Hence, only the computed turn and zigzag maneuvers are compared with the field test in this paper. The field test is carried out with a self-propulsion trimaran model powered by two water-jet impetuses. The work about the field test has been published in previous work, and the details can be found in reference (Jiang et al., 2021).



(a) trajectory of turn maneuver



(b) velocity of turn maneuver

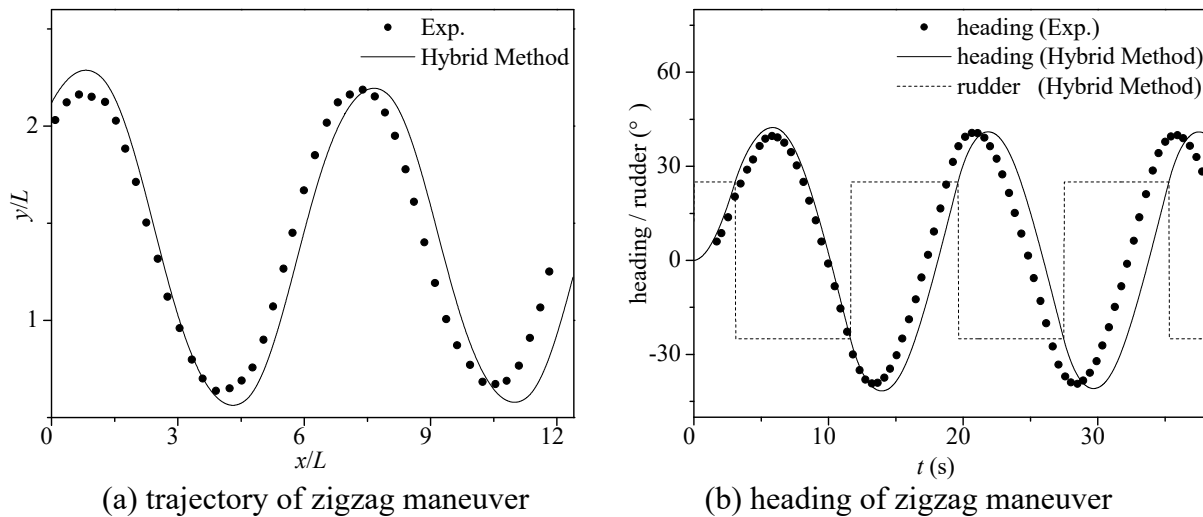


Fig. 6. Comparison between the computed and experimental results

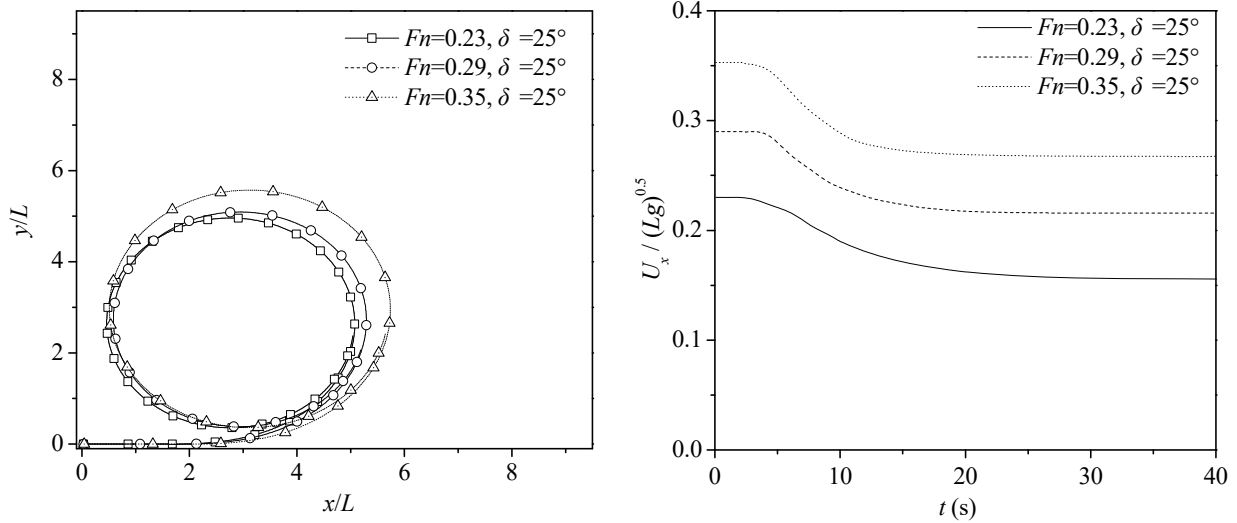
The comparison between the computed results by the current hybrid method and the field test results is shown in Fig. 6. It could be seen that the trajectory of turn and zigzag maneuver is in good agreement with the experimental results. For the turn maneuver, the main difference appears during the process of speed-down. On the other hand, for the zigzag maneuver, the computed period of bow-turning is relatively larger. The main reason for the difference is probably that the water-jet impetuses are not simulated. Therefore, the interaction between the impetus and the hull surface is not taken into consideration.

3 Results and discussions

In this section, the turn and zigzag maneuvers of the trimaran in both calm water and waves are simulated. By changing the forwarding speed and the wave parameters, the characteristics of the maneuvering are discussed.

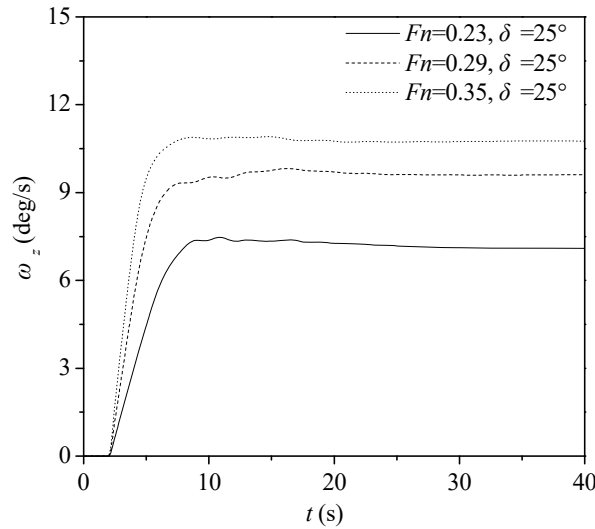
3.1 Turn and zigzag maneuvers in calm water

The same trimaran model is used for numerical simulation. The turn and zigzag maneuvers in calm water are simulated first. Three Froude numbers are used for numerical simulation, which is $Fn=0.23, 0.29,$ and $0.35,$ respectively. The rudder angle is set as $\delta=25^\circ$. At the beginning of the simulation, the trimaran moves forward at a constant speed, and the propulsion force is obtained by the simulation of moving forward in calm water. The trajectory, velocity to the x' -axis, changing heading rate, and variation of the heading and rudder angle are presented.



(a) trajectory of turn maneuver

(b) velocity of turn maneuver



(c) changing rate of heading

Fig. 7. Computed results of turn maneuver in calm water

The computed result of the turn maneuver in calm water is shown in Fig. 7. By the nondimensional trajectory in Fig. 7 (a), it could be found that the turning diameter is affected by the initial speed of the trimaran, especially when the Froude number increases from 0.29 to 0.35, the turning diameter increases from $4.7L$ to $5.3L$, about 13% larger. However, when the Froude number increases from 0.23 to 0.29, the turning diameters increase 2% from $4.6L$ to $4.7L$. Fig. 7 (b) shows that the velocity decrease is similar at different initial speeds. Still, the larger Froude number will decrease the velocity more sharply. It takes about 16.47s, 12.55s, and 11.99s to reach a stable velocity at $Fn=0.23$, 0.29, and 0.35, respectively. Combining Fig. 7 (b) and (c) shows that the changing rate of heading increases more noticeably from $Fn=0.23$ to $Fn=0.29$, which means that the turning period decreases faster at a low Froude number. It could probably be deduced that, though the turning diameter is increased, the larger speed will also increase the forward speed and heading rate during

the process of turn maneuver.

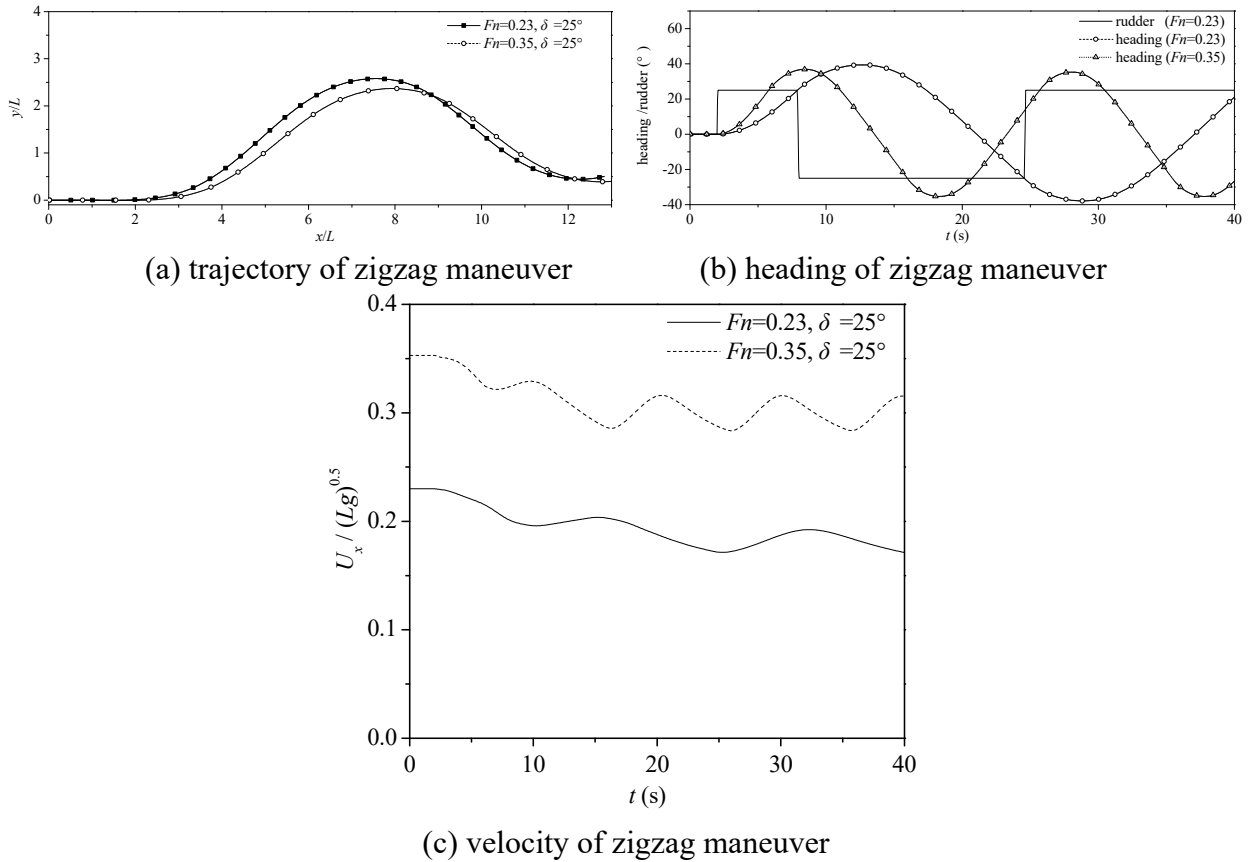


Fig. 8. Computed results of zigzag maneuver in calm water

Fig. 8 shows the zigzag maneuver of the trimaran in calm water at different speeds. It could be seen that the influence of the initial Froude number on the trajectory of the zigzag maneuver is less obvious. The y -direction offset of the trajectory is relatively more significant when the Froude number increase from 0.23 to 0.35. Fig. 8 (b) shows the steering performance of the trimaran at different speeds. The first overshoot angle and the second overshoot angle are 39.4° and 36.9° for $Fn=0.23$, and that for $Fn=0.35$ are 37.8° and 35.3° . It could be seen that the higher initial speed could decrease the overshoot angle by about 4%. However, the changes look not obvious in Fig. 8 (b), which still means the steering performance of the trimaran is relatively better at higher speeds. Both Fig. 8 (b) and (c) show that the forwarding speed will significantly affect the period of zigzag maneuver. When the Fn increases from 0.23 to 0.35, the initial turning time decreases from 5.9s to 3.8s by 35.6%, and the time of the complete cycle decreases from 35.0s to 21.3s by 39.1%.

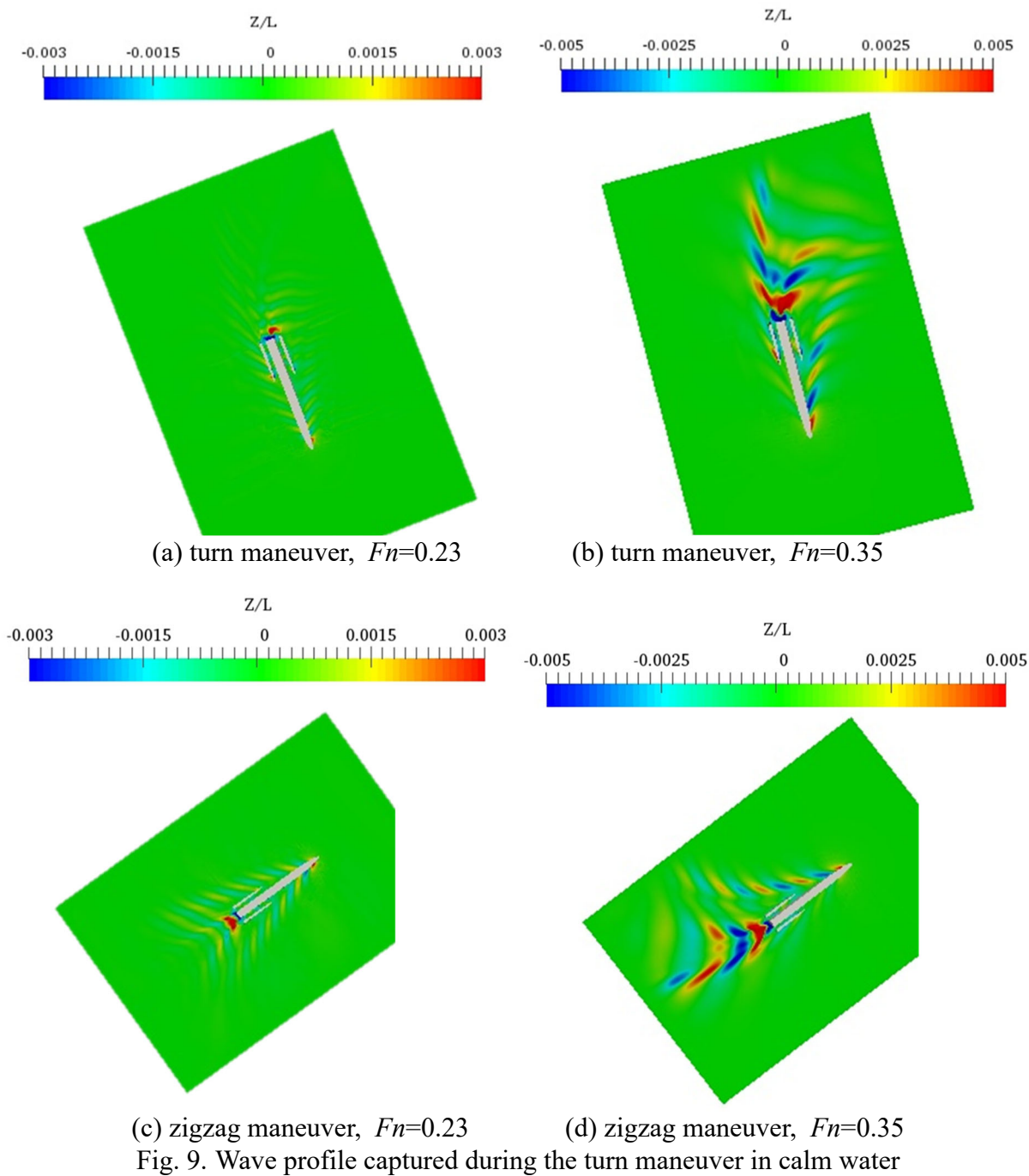


Fig. 9. Wave profile captured during the turn maneuver in calm water

Fig. 9 shows the wave profile captured during the turn and zigzag maneuvers of the trimaran in calm waters. The figures of different Fn are captured at the same headings. The flow around the hull surface is more asymmetric when the speed of the ship increases. Especially for the zigzag maneuver, when the speed is low enough, the changing rate of heading is also low. Hence, the flow disturbance by the motion of the ship is almost symmetric. When the speed is as large as $Fn=0.35$, there is almost no flow disturbance outside the turning circle.

3.2 Turn and zigzag maneuvers in waves

The turn and zigzag maneuvers of the same trimaran model in incident waves are simulated in

this section. At the beginning of the simulation, the trimaran moves forward in the head waves with rudder angle set as 0° , and the propulsion force is the same as that in calm water. After 4.0 seconds, the turn and zigzag maneuvers begin. In this paper, five different wavelengths are used for numerical simulation. During the numerical simulation process, the effect of the waves on the water-jet impetus is not taken into account in this study.

Table 1

The side-hull positions of different layouts

Case	Fn	λ/L	ak	β_0	δ	maneuver
1	0.35	0.88	0.058	180°	25°	turn / zigzag
2		1.47				
3		1.67				
4		1.09	0.058			
5			0.096			
6			0.135			

The working condition is as shown in Table 1. The $Fn=0.35$ is chosen as the initial forwarding speed, corresponding to the trimaran's designed speed. The effect of the initial wave heading on maneuverability is not studied in this paper. Hence, the initial wave heading β_0 is 180° for all the cases, which represents the head wave in this paper. For each case, the turn maneuver with the rudder angle $\delta=25^\circ$ and $25^\circ/25^\circ$ zigzag maneuver are simulated. Four wavelengths and three wave steepness are simulated to study the performance of the turn and zigzag maneuvers of the trimaran in waves of different lengths and steepness. The turn and zigzag maneuvers in different wavelengths are simulated first. The computed results are shown from Fig. 10 to Fig. 19.

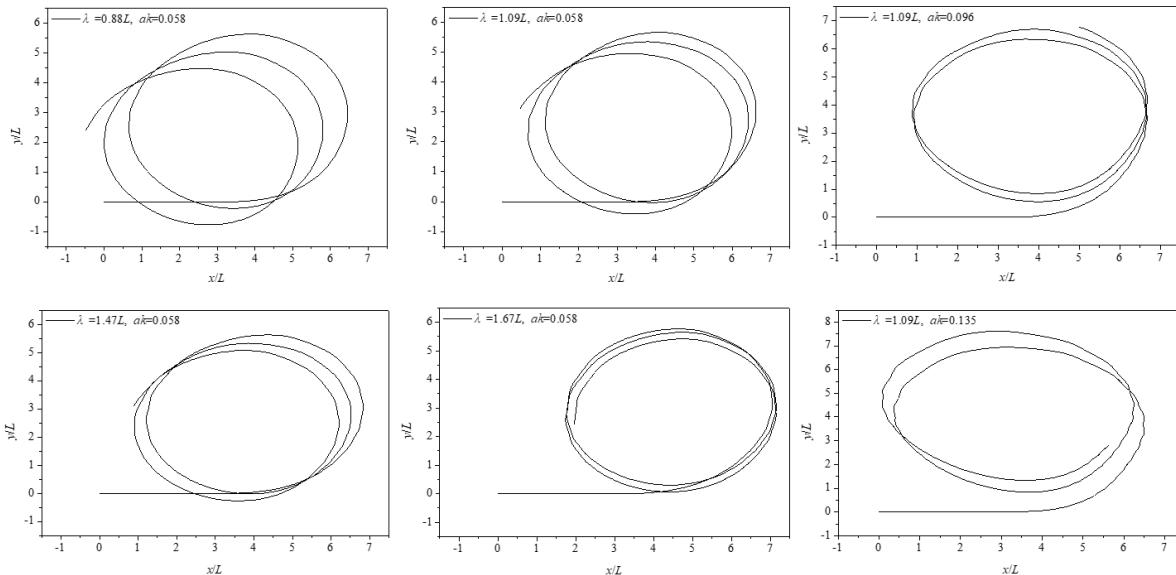
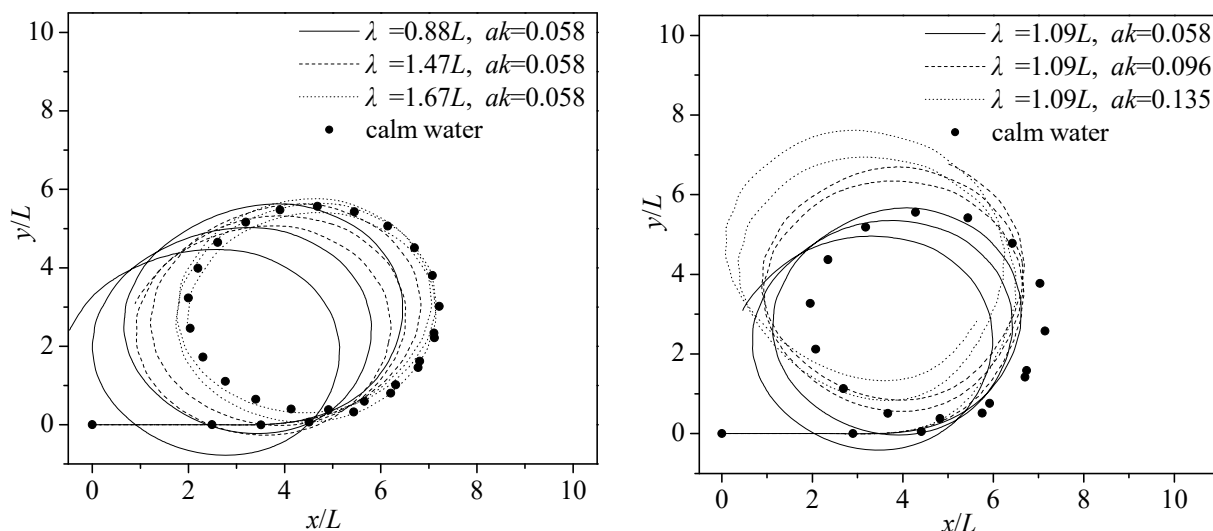


Fig. 10. Computed trajectory of turn maneuver in waves

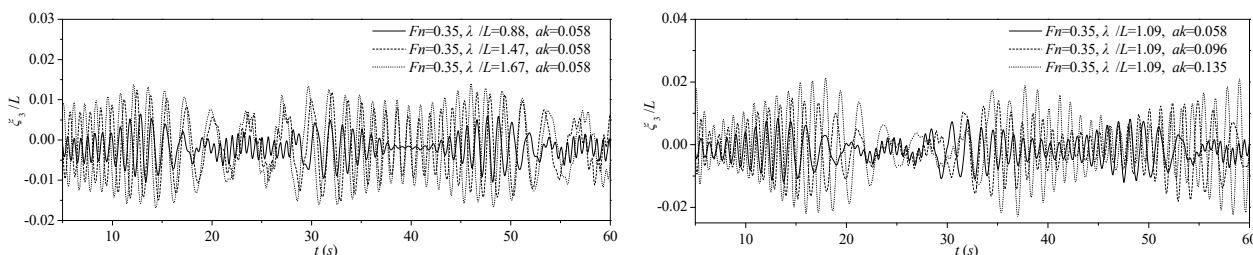


(a) various wavelengths

(b) various wave steepness

Fig. 11. Comparison between the turning trajectory in waves and calm water

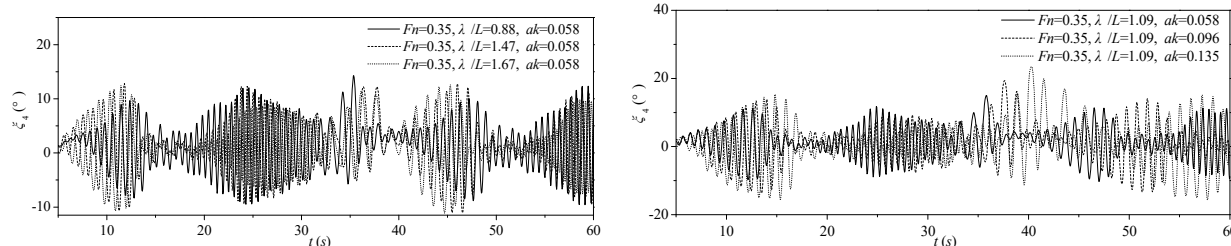
The computed trajectory of turn maneuver in waves is shown in Fig. 10 and Fig. 11. The apparent drift of the turning trajectory could be seen when the trimaran is moving in the waves, and the parameters of incident waves could significantly influence the turn maneuver of the trimaran. Fig. 11 (a) shows that the variation of the wave steepness will not change the offset direction of the turning trajectory. However, in the range of the used wavelengths, the shorter wavelength will lead to a larger offset distance. By comparing Fig. 11 (a) and (b), we could find that the influence of the wave steepness is different from the wavelength, and the wave steepness could make the offset direction of the turning trajectory vary. It is probably because the nonlinear phenomenon is more frequent in larger wave steepness, such as wave slamming, green water, and intermittent emergence of the side hulls.



(a) heave in various wavelengths

(b) heave in various wave steepness

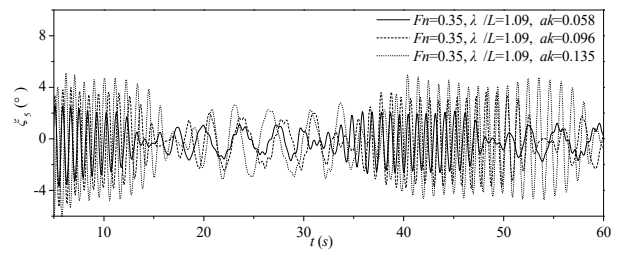
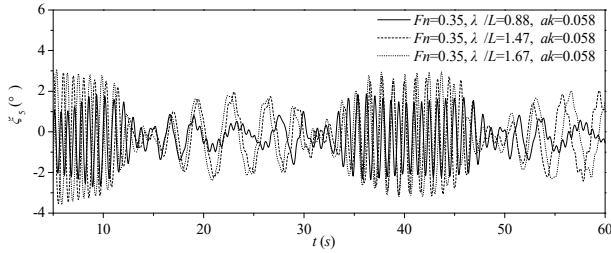
Fig. 12. Computed time history of heave motion during the turn maneuver in waves



(a) roll in various wavelengths

(b) roll in various wave steepness

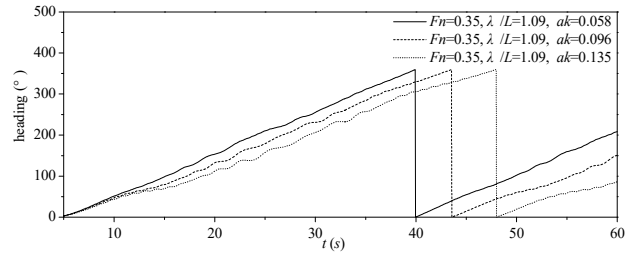
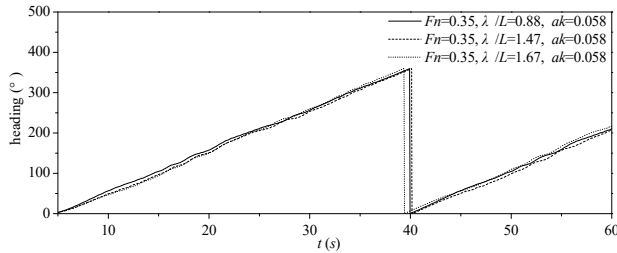
Fig. 13. Computed time history of roll during the turn maneuver in waves



(a) pitch in various wavelengths

(b) pitch in various wave steepness

Fig. 14. Computed time history of pitch during the turn maneuver in waves

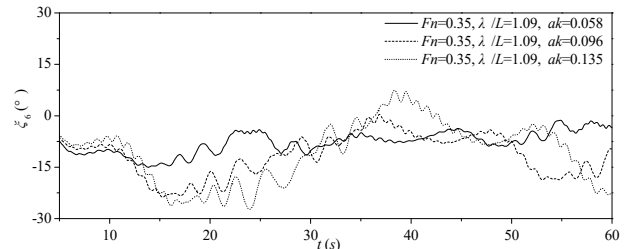
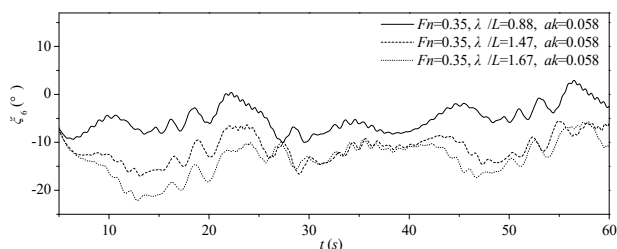


(a) heading in various wavelengths

(b) heading in various wave steepness

Fig. 15. Computed time history of heading during the turn maneuver in waves

Fig. 12, Fig. 13, and Fig. 14 show the heave, roll, and pitch motion of the trimaran during the process of turn maneuver, and Fig. 15 shows the heading. The figures show that the period and amplitude of the motion vary with the heading of the ship. Comparing the effect of the wavelength and the wave steepness shows that both the wavelength and the wave steepness could influence the amplitude of the motion during turn maneuver, which is similar to the seakeeping prediction (Gong et al., 2021a). The effect of wave steepness is relatively more significant, which could lead to larger motion amplitude. But, the heave, roll, and pitch motion phases are less affected by the wavelength, which means the turning period and heading variation is not obvious in different wavelengths. It is mainly because the offset direction is almost the same in a different wavelength, as shown in Fig. 11 (a). For the motion in different wave steepness, the phase of the motion changes obviously in different wave steepness. Combined Fig. 11 (b) with Fig. 12(b), Fig. 13(b), and Fig. 14(b), we could see that the heading and the changing rate of heading are affected by the wave steepness, and the changing rate of heading decreases with the wave steepness getting larger.



(a) yaw in various wavelengths (b) yaw in various wave steepness
 Fig. 16. Computed time history of yaw during the turn maneuver in waves

Fig. 16 is the yaw of the trimaran during the turn maneuver in waves. The time history of yaw $\xi_6(t)$ in this paper is obtained by $\xi_6(t)=r(t)-\bar{r}t$, where t is the time, $r(t)$ is the heading of the trimaran, \bar{r} is the average changing rate of heading during the turn maneuver. From Fig. 16, we could find that the wavelength could influence the average position of the yaw, but the larger wave amplitude could increase the maximum yaw value with little effect on the average yaw.

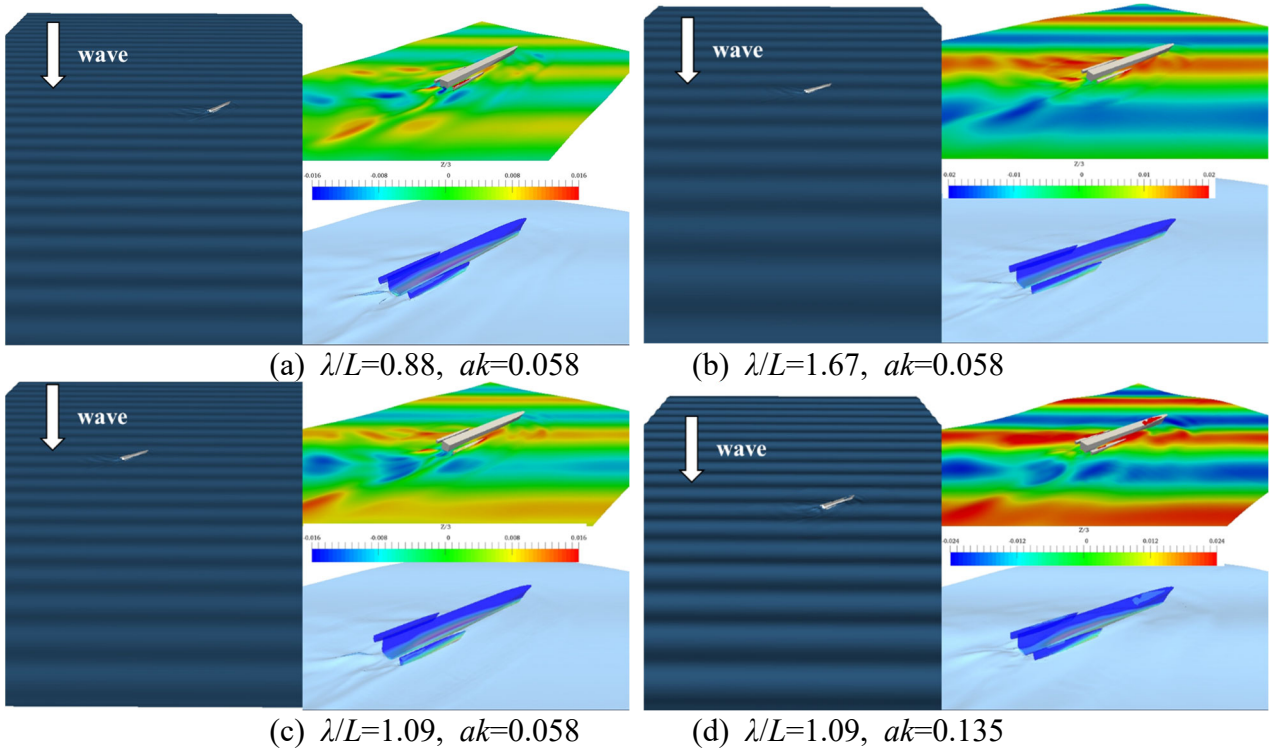


Fig. 17. Wave profile of turn maneuver in waves

Fig. 17 shows the wave profile of the turn maneuver when β is an oblique head wave, where Fig. 17 (a)(b) are cases of different wavelengths, Fig. 17 (c)(d) are of different wave steepness. It could be seen that the motion during the maneuver could lead to noticeable flow disturbance around the ship, even near the bow side. The making-wave by the pitch-roll coupling motion and the intermittent emergence of the side hulls could be observed. Comparing Fig. 17 (a) and (b), it could be found that, though the wave amplitude is small in Fig. 17 (a), the high wave frequency will also lead to significant roll motion during the turn maneuver, which could also be seen in Fig. 14 (a). The green water of the side hull is obvious in Fig. 17 (a). The effect of the wave steepness is shown in Fig. 17 (c)(d). Though the wavelength is the same, the increase of the wave amplitude will lead to the variation of the draft during the turn maneuver, which will lead to the larger wetted surface area, lifting surface area, and pressure distribution. In Fig. 17 (d), the green water could be seen on both

the center and side hull.

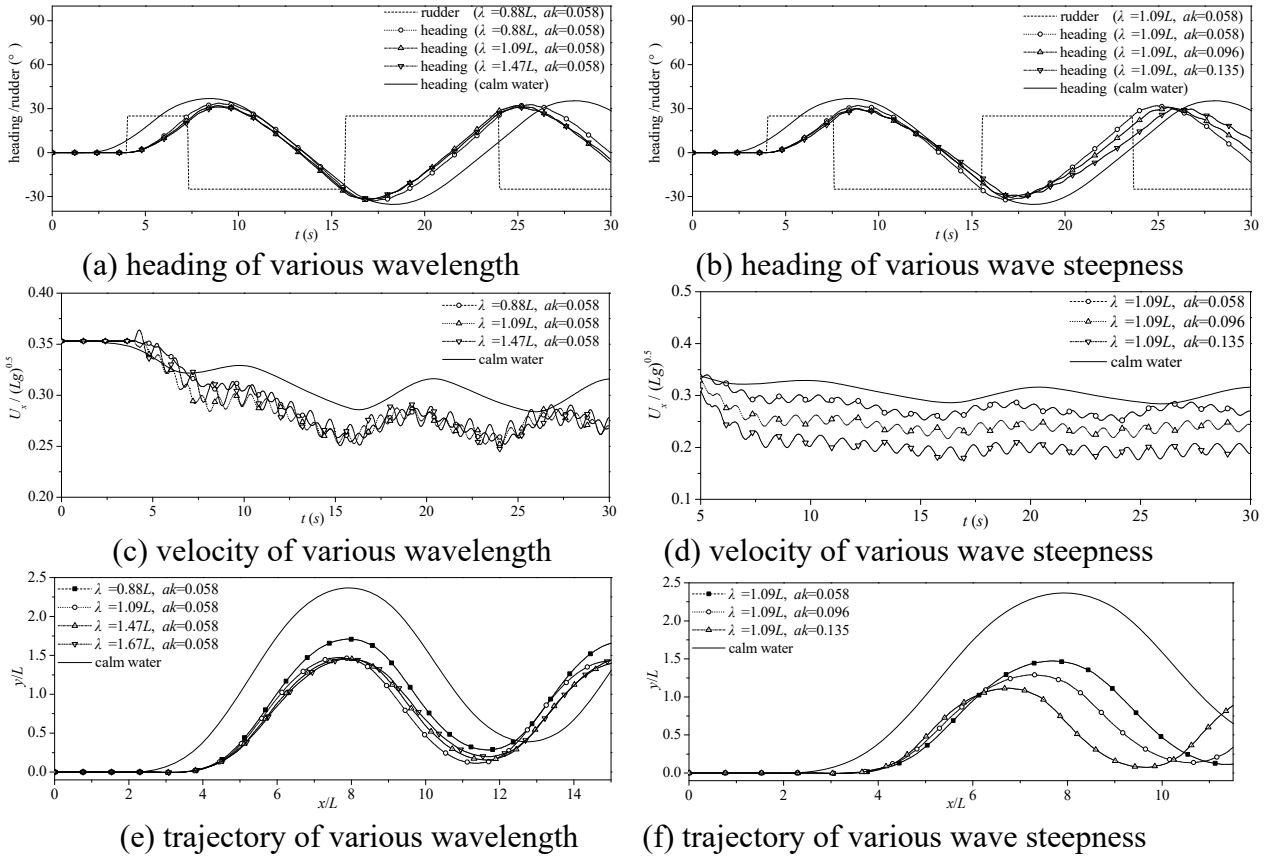
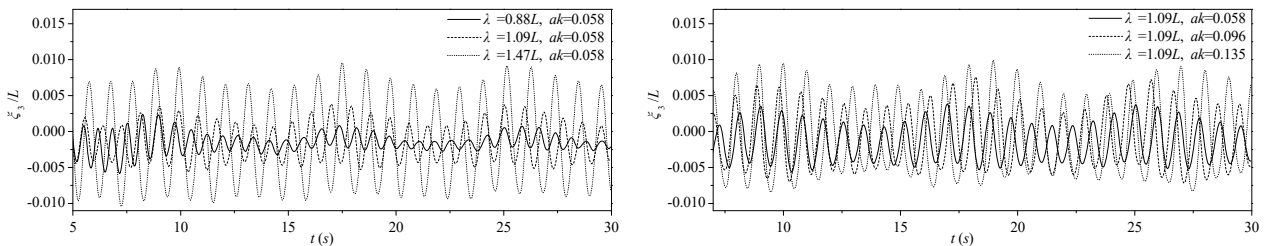


Fig. 18. Computed heading, velocity, and trajectory of zigzag maneuver in waves

Fig. 18 shows the computed results of the zigzag maneuver in waves, including the heading, velocity to the stem direction, and the moving trajectory in the xy -plane. By comparing Fig. 18 with Fig. 11, it could be noticed that the trajectory of the zigzag maneuver is significantly affected by the incident waves. The difference between the trajectory of zigzag maneuver in waves and calm water is noticeable, compared with that of turn maneuver. The main reason is that, when carrying out zigzag maneuvers in waves, the trimaran will always move in the waves ranging from head waves to oblique head waves. In such wave headings, the added resistance can be increased, and the trimaran's forward speed can be reduced to a large extent, as shown in Fig. 18 (d). From Fig. 18 (b)(f), it also could be found that the larger wave amplitude will make the moving forward of the trimaran slower, and the effect of wave amplitude on the zigzag maneuver is more significant than the wavelength.



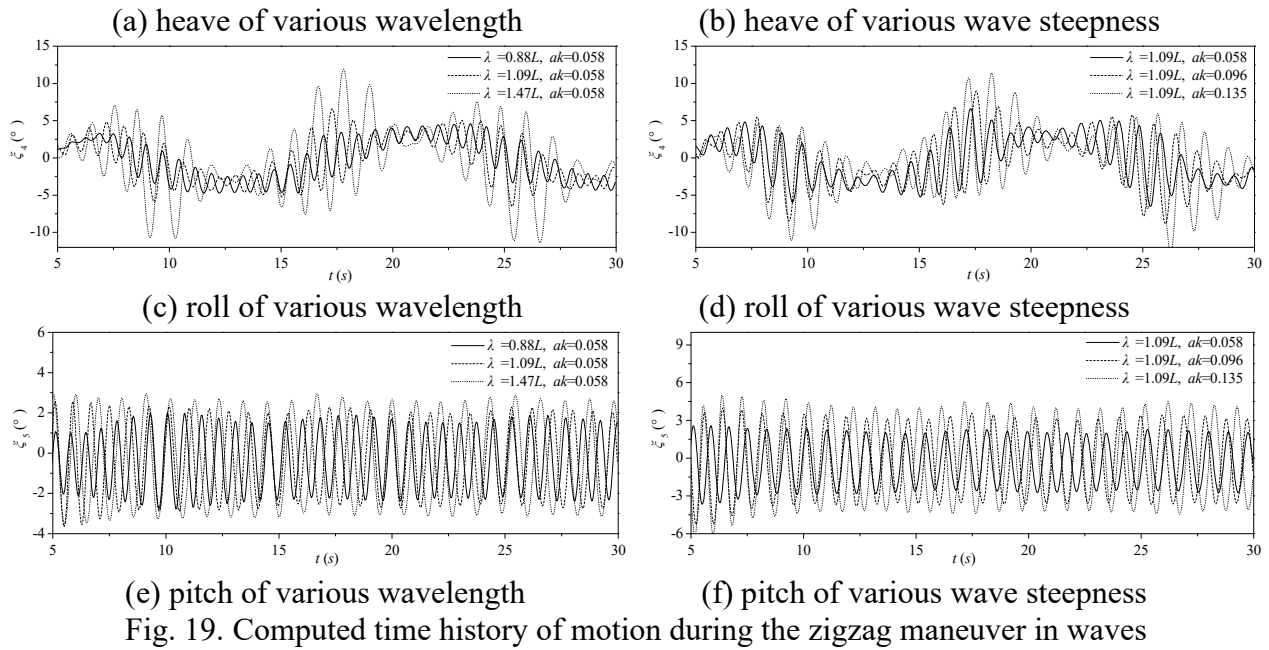
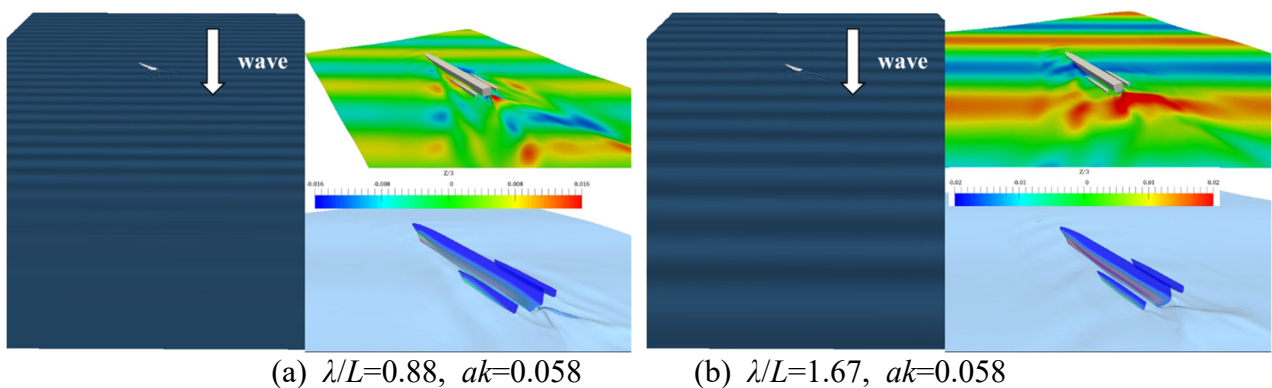
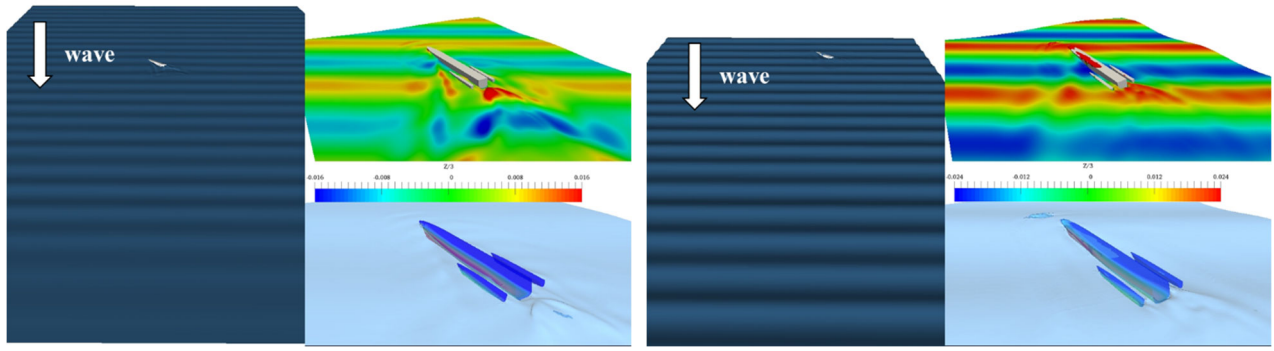


Fig. 19 shows the motion time history of the trimaran in waves during the zigzag maneuver.

The motion of the trimaran during the zigzag maneuver in waves is shown in Fig. 19. Because the trimaran's heading varies in the scope of -40° to $+40^\circ$, the trimaran moves in oblique head waves during the zigzag maneuver. In such a range of wave heading, both the wavelength and wave steepness could significantly influence the ship's motion. Especially for the heave and roll motion, the increase of both the wavelength and wave steepness will lead to more significant heave and roll motion. The difference is that when the wavelength gets shorter, the heave and roll motion will decrease faster, as shown in Fig. 19 (a)(c). However, the phenomenon is different for the pitch motion. The pitch motion decreases more noticeably when the wave steepness gets smaller. By comparing the heave, pitch motion with the roll motion, we could find that when the trimaran is carrying out the zigzag maneuver, the variation of the pitch amplitude is not noticeable. But, the variation of the heave amplitude is evident, and the roll amplitude could change significantly at a different time step.





(c) $\lambda/L=1.09$, $ak=0.058$ (d) $\lambda/L=1.09$, $ak=0.135$
 Fig. 20. Wave profile of zigzag maneuver in waves

Fig. 20 shows the wave profile captured when the largest heading of the zigzag maneuver occurs. Fig. 20 (a)(b) are the wave profile at the same heading in different wavelengths, and Fig. 20 (c)(d) are wave profiles at the same heading in different wave steepness. The trimaran is always moving in oblique head waves with $145^\circ \leq \beta \leq 180^\circ$, the coupling of pitch and roll motion is not as significant as that of turn maneuver, and the green water could be only found on the center hull as shown in Fig. 20 (d). Hence, compared with the turn maneuver, the wave disturbance of the zigzag maneuver is less noticeable. However, the wave steepness will significantly influence the longitudinal pressure distribution on the center hull. Fig. 20 (d) shows that the severe pitch motion, green water, and bow diving will happen during the zigzag maneuver.

4 Conclusion

In this paper, a hybrid method coupling the FNPT-based QALE-FEM and viscous flow method is applied to simulate the turn and zigzag maneuvers of trimaran in both calm water and waves. The numerical tank is simulated in the external domain by FNPT and QALE-FEM, and the maneuver and motion of the trimaran are realized in the internal domain by viscous flow theory. The interaction between the fluid and the ship motion, the nonlinear motion of trimaran, and the intermittent emergence of side hulls during the maneuver are considered. With the computed results of turn and zigzag maneuvers of the trimaran, the following conclusion could be drawn.

1) The turning diameter of the trimaran is affected by the initial speed, and the larger speed will make the turning diameter increase obviously, and the turning period is much smaller. The influence of the initial speed on the trajectory of the zigzag maneuver in calm water is less obvious, and the steering performance of the trimaran is relatively better at a higher speed.

2) The turning maneuver of the trimaran in waves is significantly affected by the wavelength and wave steepness. The wavelength could change the offset distance of trimaran in waves, but the

1
2 356 wave steepness could influence the offset direction of the trimaran.

3
4 357 3) The wavelength has relatively little influence on the trajectory and heading of the zigzag
5
6 358 maneuver of the trimaran in waves. But the wave steepness could make the zigzag maneuver changes
7
8 359 significantly by slowing down the forward speed of the trimaran.

9
10 360 4) For the motion during the maneuver, the condition of the waves could make the motion of the
11
12 361 zigzag maneuver changes obviously, because the trimaran is always moving in oblique head waves.
13
14 362 The effect of the wave parameters on motion amplitude is less noticeable during turn maneuver, but
15
16 363 the phase of the motion time history could be different in different wave steepness.

17
18 364

19

20 365 **Acknowledgement**

21

22

23 366 This project was supported by the Natural Science Foundation of Shanghai, China (grant
24
25 367 19ZR1422500), National Natural Science Foundation of China (grant 51979157).

26
27 368

28

29 369

30

31

32 370

33

34 371

35

36 372

37

38 373

39 374

40

41 375

42

43 376

44

45 377

46

47 378

48

49 379

50

51 380

52

53 381

54

55 382

56

57 383

58

59 384

60

61 385

62 386

63

64

65

66

67

68

69

70

71

72

73

74

75

76

77

78

79

80

81

82

83

84

85

86

87

88

89

90

91

92

93

94

95

96

97

98

99

100

101

102

103

104

105

106

107

108

109

110

111

112

113

114

115

116

117

118

119

120

121

122

123

124

125

126

127

128

129

130

131

132

133

134

135

136

137

138

139

140

141

142

143

144

145

146

147

148

149

150

151

152

153

154

155

156

157

158

159

160

161

162

163

164

165

166

167

168

169

170

171

172

173

174

175

176

177

178

179

180

181

182

183

184

185

186

187

188

189

190

191

192

193

194

195

196

197

198

199

200

201

202

203

204

205

206

207

208

209

210

211

212

213

214

215

216

217

218

219

220

221

222

223

224

225

226

227

228

229

230

231

232

233

234

235

236

237

238

239

240

241

242

243

244

245

246

247

248

249

250

251

252

253

254

255

256

257

258

259

260

261

262

263

264

265

266

267

268

269

270

271

272

273

274

275

276

277

278

279

280

281

282

283

284

285

286

287

288

289

290

291

292

293

294

295

296

297

298

299

300

301

302

303

304

305

306

307

308

309

310

311

312

313

314

315

316

317

318

319

320

321

322

323

324

325

326

327

328

329

330

331

332

333

334

335

336

337

338

339

340

341

342

343

344

345

346

347

348

349

350

351

352

353

354

355

-
- 388 military trimaran hull by a novel overset mesh method in regular and irregular waves.
389 Scientific Journals of the Maritime University of Szczecin, 65(137).
- 390 Gong, J. Y., Li, Y. B., Jiang, F., Hong, Z. C., and Yu, D., 2019. Maneuvering Simulation and
391 Study on the Effect of Hull Attitude on Maneuverability of Trimarans by OpenFOAM. Journal
392 of Coastal Research 36(1), 157-173.
- 393 Gong, J. Y., Li, Y. B., and Jiang, F., 2020a. Numerical simulation about the manoeuvre of trimaran
394 and asymmetric twin hull with hull attitude taken into account by OpenFOAM. Journal of
395 Marine Science and Technology, 25(3), 769-786.
- 396 Gong, J. Y., Yan, S. Q., Ma, Q. W., and Li, Y. B., 2020b. Added resistance and seakeeping
397 performance of trimarans in oblique waves. Ocean Engineering, 216, 107721.
- 398 Gong, J. Y., Li, Y. B., Fu, Z., Li, A., and Jiang, F., 2021a. Study on the characteristics of trimaran
399 seakeeping performance at various speeds. Journal of the Brazilian Society of Mechanical
400 Sciences and Engineering, 43(4), 194.
- 401 Gong, J. Y., Yan, S. Q., Ma, Q. W., and Li, Y. B., 2021b. Numerical simulation of fixed and
402 moving cylinders in focusing wave by a hybrid method coupling QALE-FEM with
403 OpenFOAM. International Journal of Offshore and Polar Engineering, 31(1), 102-111.
- 404 Javanmardi, M. R., Jahanbakhsh, E., Seif, M.S., and Sayyaadi, H., 2008. Hydrodynamic analysis of
405 trimaran vessels. Polish Maritime Research 15, 11-18.
- 406 Jiang, F., Li, Y. B., and Gong, J. Y., 2021. Study on the manoeuvre characteristics of a trimaran
407 under different layouts by water-jet self-propulsion model test. Applied Ocean Research, 108(2),
408 102550.
- 409 Jong, P. D., Renilson, M., and Walree, F. V., 2012. The broaching of a fast rescue craft in following
410 seas. Proceedings of the 12th International Conference on Fast Sea Transportation, FAST2013,
411 Amsterdam, The Netherlands.
- 412 Katayama, T., Taniguchi, T., Fujii, H., and Ikeda, Y., 2009. Development of maneuvering
413 simulation method for high speed craft using hydrodynamic forces obtained from model tests.
414 10th International Conference on Fast Sea Transportation FAST 2009, Athens, Greece.
- 415 Li, Y., and Lu, X., 2007. An investigation on the resistance of high speed trimaran. Journal of Ship
416 Mechanics, 11(2), 191-198.
- 417 Li, Q., Wang, J. H., Yan, S. Q., Gong, J. Y., and Ma, Q. W., 2018. A zonal hybrid approach coupling
418 FNPT with OpenFOAM for modelling wave-structure interactions with action of current. Ocean
419 Systems Engineering, 8(4), 381-407.
- 420 Nowruzli, L., Enshaei, H., Lavroff, J., Kianejad, S. S., and Davis, M. R., 2020. CFD simulation of
421 motion response of a trimaran in regular head waves. The International Journal of Maritime
422

422 Engineering, 162(A1), 91-106.
2
423 Onas, A., and Datla, R., 2011. Non-linear roll motions of a frigate-type trimaran. Proceedings of the
4
424 11th International Conference on Fast Sea Transportation, 26-29.
5
425 Roache, P. J., 1994. Perspective: a method for uniform reporting of grid refinement studies. Journal
7
426 of Fluids Engineering, 116(3), 405-413.
9
1027 Wang, S. M., Duan, W. Y., Xu, Q. L., Duan, F., Deng, G. Z., and Li Y., 2021. Study on fast
11
1028 interference wave resistance optimization method for trimaran outrigger layout. Ocean
13
1029 Engineering, 232(6), 109104.
14
1530 Yasukawa, H., Hirata, N., and Kose, K., 2005. Influence of outrigger position on the performances
16
1031 of a high speed trimaran. The Japan Society of Naval Architects and Ocean Engineers, 2, 197-
18
1032 203.
20
21
22
23
24
25
26
27
28
29
30
31
32
33
34
35
36
37
38
39
40
41
42
43
44
45
46
47
48
49
50
51
52
53
54
55
56
57
58
59
60
61
62
63
64
65